

# Point contact diode at laser frequencies

K. M. Evenson, M. Inguscio,<sup>a)</sup> and D. A. Jennings

*Time and Frequency Division, National Bureau of Standards, Boulder, Colorado 80303*

(Received 21 November 1983; accepted for publication 4 June 1984)

Dramatic improvements in the stability of the metal-insulator-metal point contact diode has been achieved by the use of blunter whisker tips. The optimum values for tip radius and diode resistance were experimentally determined. Both sensitivity and high-speed response of W-NiO-Ni point contact diodes were investigated at different laser frequencies and mixing orders as a function of tip radius, resistance, and coupling. The tip radii were changed by more than an order of magnitude, and surprisingly, the sensitivity and the harmonic generation up to 88 THz were not significantly affected. A conical antenna was found to be superior to the conventional long-wire antenna at wavelengths shorter than  $10\ \mu\text{m}$ . Responsivity measurements as a function of the diode resistance showed evidence for two different physical mechanisms responsible for the operation of the diode.

## INTRODUCTION

Metal-insulator-metal (MIM) diodes in point contact configuration have been used extensively for absolute measurements of laser frequencies from the far infrared to the visible.<sup>1</sup> Electron tunneling is the most widely accepted explanation for their extremely broadband response.<sup>2-6</sup> However, there is evidence for more than one phenomenon occurring in the diode; this other phenomenon may contribute to opposite polarity video detection at visible wavelengths.<sup>7</sup> Most experiments and theories have indicated that the contact area should be as small as possible in order to decrease the capacitance and hence minimize the response time. Consequently, tip radii in the 40–90-nm range have been generally used. These sharp tips detrimentally affect the mechanical stability of the diodes. Also, delicate and short-lived contacts can make difficult a quantitative and systematic investigation of the physical properties of the diode.

Another limitation can arise from the long-wire antenna coupling generally used. Its highly selective wavelength dependence on the angle of incidence of the radiation leads to somewhat complicated geometries when different wavelengths must be coupled to the diode for multiple radiation mixing experiments.

In this paper we report results of a systematic investigation of the behavior of W-NiO-Ni point contact diodes at different laser frequencies and mixing orders with diodes having different tip radii. Coupling via a conical antenna was also investigated.

## THE DIODE

Three different nickel bases were used: polycrystalline Ni surfaces either (a) polished, or (b) polished and etched, and (c) a polished Ni surface with a vapor deposited Ni overlay 200 nm in thickness. No significant differences were observed between the various bases, and the vapor deposited surface was used for most of the measurements. This configuration was chosen in order to have an optically flat and

uniform surface. Moreover, this deposited surface showed no irregularities under electron microscopic examination, which indicated that the geometric characteristics of the contact were mainly determined by the whisker and could be controlled by the shape of the tungsten tip.

The whiskers were produced by electrically etching a  $25\text{-}\mu\text{m}$ -diam tungsten wire in NaOH. Long-wire antennae which we use typically have conical tips of about  $25^\circ$ , but  $40^\circ$ – $50^\circ$  conical tips were produced to check conical coupling. These blunt conical tips were formed by maintaining the upper contact position of the etchant solution fixed by carefully lowering the antenna during the etching process. This technique does not produce uniform antennae, and a large fraction of the antennae were discarded. The height  $H$  of the cone ranged between 15 and  $70\ \mu\text{m}$  and the angle could be varied between  $17^\circ$  and  $60^\circ$ . The tip radii ranged between 50 and 1300 nm. In general, different whiskers were used for each cone shape, but sometimes we etched the same whisker more than once in order to vary only the tip radii, keeping constant the other parameters such as angle and height of the cone and length of the wire. Each diode was examined with an electron microscope. Typical pictures in Fig. 1 show (a) the same cone which was reetched three times to obtain tip radii of (b) 50 nm, (c) 94 nm, and (d) 170 nm. Generally, we took electron microscope pictures of the tips before and after contact with the nickel to investigate possible modifications during use.

Radiation patterns were measured for long-wire and conical antennae and are shown in Fig. 2. For these angular dependence measurements, a "plane wave" was approximated by focusing the radiation from a  $\text{CO}_2$  laser (about 30 mW) with a long-focal-length lens which provided a beam convergence of less than  $2^\circ$ . The long-wire pattern is shown in Fig. 2(a). This antenna had a rounded transition between the cone and the wire, and had a diameter of  $12\ \mu\text{m}$ , a total length  $L = 0.2\ \text{mm}$ , a cone height  $H = 20\ \mu\text{m}$ , angle  $\alpha = 30^\circ$ , and a tip radius of 250 nm. The number of lobes and the angular position of the first maximum are approximately consistent with the predictions of traveling-wave theory<sup>8</sup> and show that the pattern of the radiation agrees with an effective antenna length corresponding to the length from the tip to the bend of the whisker.

<sup>a)</sup> Permanent address: Dipartimento di Fisica, Piazza Torricelli, 2, I-56100 Pisa, Italy.

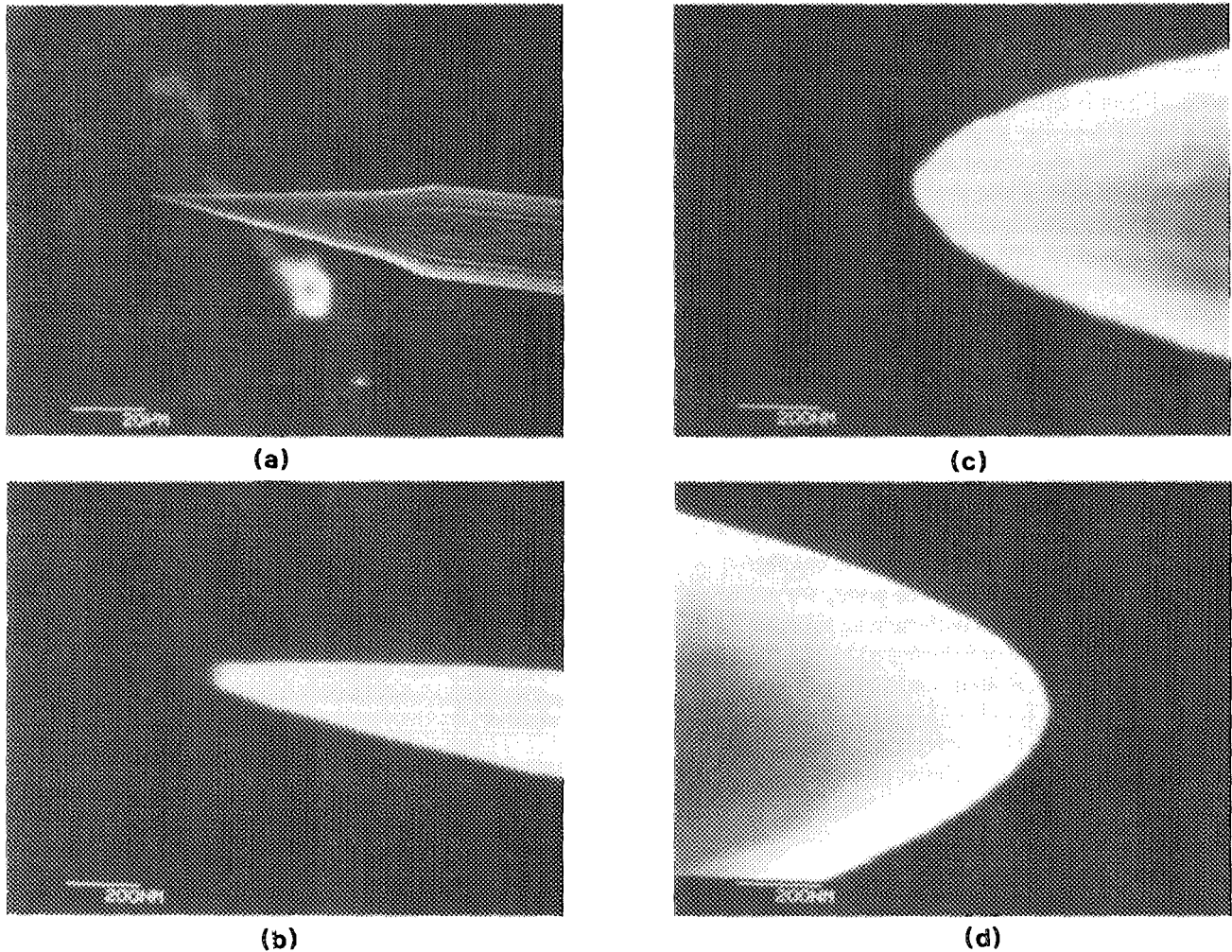


FIG. 1. Electron microscope pictures of one of the tungsten conical whiskers and some different tips used in the experiments. The scale is given in the lower left-hand corner of each picture.

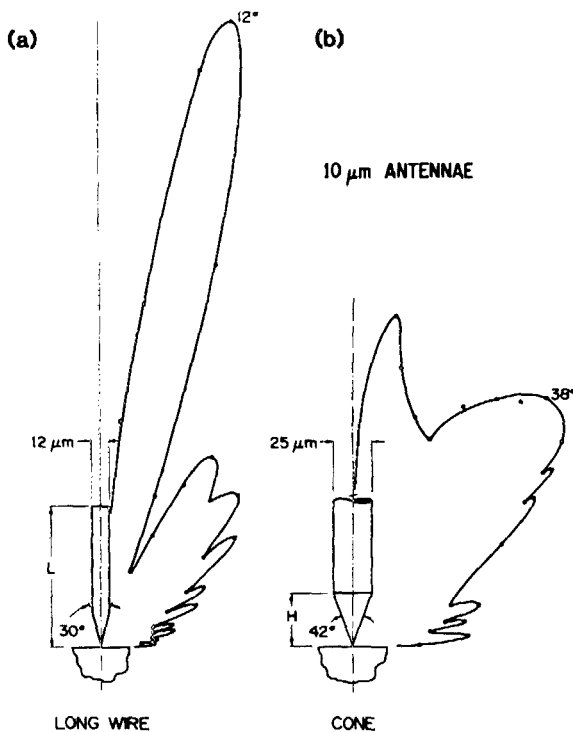


FIG. 2. Comparison between the antenna pattern of (a) a conventional long-wire point contact diode, and (b) a conical point contact diode.

The conical pattern is shown in Fig. 2 (b) for a tip radius of 150 nm. Use of the conical antenna at laser frequencies was first reported in 1973 at 29 and 88 THz.<sup>9</sup> Improved focusing with the use of the parabolic mirror seems to increase the coupling to the conical antenna, especially as frequencies approach the visible. In contrast with conventional long-wire coupling, strong angular dependence was absent for the conical coupling at 10  $\mu\text{m}$ . Instead of the many narrow lobes of alternating phase typical of the long wire, the broad lobe centered around 38° was obtained. At an angle nearly perpendicular to the wire, some structure is observed in general agreement with both theory and the microwave measurements reported in Ref. 10. It is worth noting that some long-wire coupling may still be present and produces the lobe at about 8° (the length of the antenna was  $L = 5.4$  mm). By a comparison between the two patterns, it is also evident that for the long wire in Fig 2 (a) some conical coupling was also present. The secondary maxima pattern, in fact, does not have the contrast and sharpness typical of pure long-wire operation. However, this effect could be partially caused by the 2° focusing of the laser radiation. As for the relative efficiency of the two couplings, conical and long

wire, it should be noted that the maximum detectivity at 10  $\mu\text{m}$  with the long wire was several times better than with the cone. However, the cone response was improved by use of shorter-focal-length optics, and the long wire was degraded because a larger focusing angle overlaps minor lobes with opposite polarity. With a 9-mm-focal-length off-axis parabola at 45°, conical coupling was nearly an order of magnitude better than the long-wire coupling.

All laser beams (at 170.6, 127, 10.2, and 3.39  $\mu\text{m}$ ) used in the video detection, mixing, and harmonic generation experiments were focused on the diodes with the 9-mm-focal-length parabolic mirror. The beam was reflected 90° by the parabola. The focused radiation was incident at 45° with respect to the whisker with *p*-type polarization in the plane formed by the wire and the beam direction.

### TIP RADIUS EFFECT: THIRD HARMONIC GENERATION

Encouraged by a chance measurement at infrared frequencies in which video signals were almost unaffected by a large decrease in the sharpness of the point, we performed high-frequency tests on diodes with varying tip radii. In this experiment, differing tip radii were tested by the generation of third harmonic signals. Radiations from a 3.39- $\mu\text{m}$  He-Ne laser at 88 THz, from a  $R_1(30)$  CO<sub>2</sub> laser emission at 29.3 THz, and from a 48.7-GHz klystron were focused on the diode with coupling and geometries as previously described. The heterodyne signal of a few tens of megahertz was produced by the difference of the third harmonic of the CO<sub>2</sub> laser and the first harmonic of the He-Ne laser and the klystron. After amplification in a broadband amplifier, the beat note with signal-to-noise (S/N) ratios up to 25-30 dB could be observed on a spectrum analyzer. The power focused on the diode was 30 mW from each of the lasers. The microwave power was adjusted to be close to the saturation power for the diode. The S/N ratio of the heterodyne signal was measured as a function of the resistance (adjusted mechanically) for each diode. The video response at 10  $\mu\text{m}$ , 3.39  $\mu\text{m}$ , and 48 GHz was also recorded. Typically, the video signals increased almost linearly with the resistance up to about 1 k $\Omega$  and then showed some nonlinearity with the signal about 50% higher at 2 k $\Omega$  than at 1 k $\Omega$ . The responsivity varied with the wavelength and was about two orders of magnitude smaller at 3.39  $\mu\text{m}$  than at 10  $\mu\text{m}$ . With a resistance of 500  $\Omega$ , typical dc signals were 20 mV at 10  $\mu\text{m}$  and 200  $\mu\text{V}$  at 3.39  $\mu\text{m}$ . The surface of the parabolic mirror used for focusing was machined with a surface quality appropriate for operation at wavelengths greater than 100  $\mu\text{m}$ ; therefore, the decrease at 3.39  $\mu\text{m}$  is mainly due to the poor optics. The measured rectified signals were nearly constant for all tip radii between 50 and 760 nm at resistances below 1 k $\Omega$  and exhibited a small decrease (about 10%) in sensitivity for the duller diodes at higher resistance. The heterodyne S/N ratio was optimum at resistance values between 300 and 500  $\Omega$  and showed a gradual decrease of the signal at increasing resistance and a rapid decrease at lower resistances. Typical results are shown in Fig. 3. Diodes with four significantly different tip radii were used, the three sharpest being from the cone shown in Fig. 1. No significant differences in the S/N were observed between "sharp" or "dull" tips. This result is

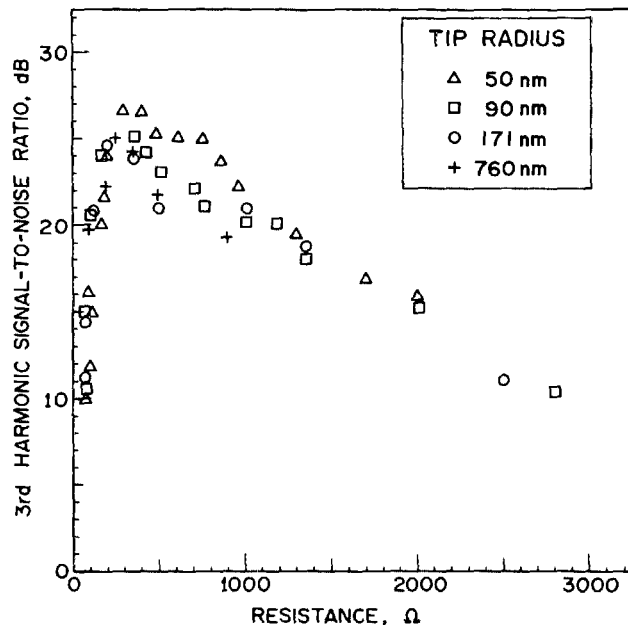


FIG. 3. Signal-to-noise ratios in a fixed bandwidth for the observed beat signals in the third-harmonic experiment as a function of the diode resistance. The beat was generated by the synthesis scheme  $\nu_B = \nu_{3.39} \mu\text{m}^{-3} \times \nu_{R(30)} - 48.7$  GHz. Results for diodes with different tip radii are reported.

quite surprising and indicates that sharp diodes are not necessary for high-speed operation. The "spreading resistance" in the base is proportional to the inverse of the contact radius. Hence, the RC time of response is proportional to the radius.<sup>9</sup> For a tip radius of a few tens of nanometers a frequency cutoff of over 100 THz is observed, and with a tip radius of several hundred nanometers a frequency cutoff nearly one order of magnitude less is predicted; in disagreement with these experimental results. It seems that the "effective contact area" may not be determined by the square of the radius of the tip. This might be partially explained by the burying of the tip into the base as reported by Sanchez *et al.*<sup>5</sup> Moreover, it is not clear how the dielectric constant of the oxide in the contact changes and affects the capacitance under the high mechanical and thermal stresses.

These results, besides stimulating questions about the theory of the mechanism of the diode, have pointed out some practical design improvements. In particular, with the use of less-sharp tips the stability of the diode has been dramatically increased without a significant decrease in the sensitivity or response times. The same contact can be stable for hours to days in normal laboratory environmental conditions without readjustment. Also, the diode resistance can be more precisely adjusted and reset with a resolution of a few tens of ohms. This is particularly important for the optimization of the heterodyne S/N ratio in harmonic generation and mixing experiments.

### TWO MECHANISMS?

The same diodes were used to perform a reproducible series of mixing experiments at different mixing orders.<sup>11</sup> The experiments were performed to measure the heterodyne signal as a function of impedance and speed of the diode. The response time is the reciprocal of the largest difference

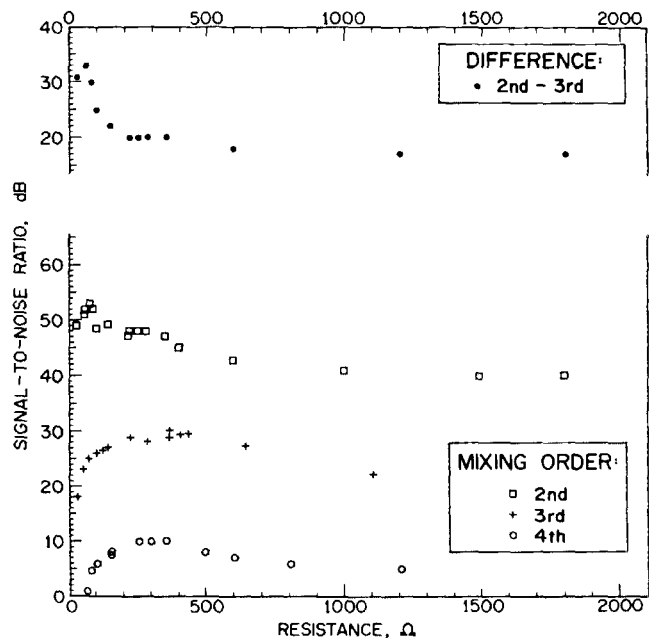


FIG. 4. Signal-to-noise ratios of the observed beat signal in different mixing order experiments as a function of diode resistance but for fixed bandwidth. The plot at the top of the figure is the difference between the results for second- and third-order mixing experiments.

( $\nu_1 - \nu_j$ ). These were sum or difference measurements without harmonic generation. The conical diode had a cone angle of  $30^\circ$  and a tip radius of about 280 nm. The results are shown in Fig. 4. The usual preamplifier was not used for the measurements because of large signal saturation effects, and the rf signal from the diode was fed directly into the spectrum analyzer; hence the signal-to-noise is many times weaker than normal. For the second-order experiment, two  $\text{CO}_2$  lasers oscillating on the same line were used, one locked near the center of the gain curve by the  $\text{CO}_2$  saturated fluorescence technique, the other with a frequency offset of about 20 MHz. Thus, in this experiment, the response frequency was 20 MHz. The power at the diode from each of the two lasers was about 30 mW. The rf difference frequency was observed over a range of resistance from  $20\Omega$  to 20 k $\Omega$ . The third-order experiment was performed by heterodyning the 170.6- $\mu\text{m}$  (1.7 THz) emission from a  $\text{CH}_3\text{OH}$  optically pumped laser with two  $\text{CO}_2$  lasers: one oscillating on  $P_1$  (36), the other on  $R_1$  (40). The response time here is ( $0.6 \times 10^{-12}$ ) sec. The powers from the two  $\text{CO}_2$  lasers were the same as in the second-order experiments. The video signal due to the far infrared laser was of the order of 1 mV at 1 k $\Omega$ . The fourth-order experiment was performed by heterodyning a 127.0- $\mu\text{m}$  (2.4 THz) line from  $^{13}\text{CD}_3\text{OH}$  (Ref. 12) with two  $\text{CO}_2$  lasers and an X-band klystron. Here, the response time is ( $0.4 \times 10^{-12}$ ) sec. Again, the power from the  $\text{CO}_2$  lasers was the same as for the other experiments. The video signal from the far infrared radiation was almost the same as for the third-order experiment. From Fig. 4 we see a loss of about 20 dB for each increase in order. More interesting is the behavior of the response as a function of the diode resistance. The third- and fourth-order mixing experiments exhibit maxima at about 300  $\Omega$  with a gradual S/N decrease at higher resistance and a rapid decrease at lower resistances, similar to the

third harmonic results in Fig. 3. In contrast, the second-order curve is quite different from those for third and fourth order. In this case, the response frequency is at 20 MHz rather than in the terahertz region as in the case of the third- and fourth-order experiments. In the top of Fig. 4 we plotted the difference between the third- and the second-order signal. This dramatic increase at lower impedances has been repeated in similar experiments recently performed at the laboratory of M. Inguscio. In this case the difference in frequency was increased to 200 MHz and similar results were observed. This difference curve represents a response that shows up below 200 MHz and must be the result of a different mechanism from those in curves 3 and 4.

This slower response could be related to the heterodyne measurements at 50  $\Omega$  plotted as a function of the frequency difference and reported in Ref. 7.

This evidence for another mechanism may help to explain the behavior of the diode at frequencies approaching the visible. Previous results show that above 200 THz the polarity of the rectified voltage (normally the tungsten is driven negative with respect to the Ni) was reversed but that a negative driven whisker was not necessary for difference generation. The slower mechanism, possibly thermal, evidenced in the measurements of Fig. 4, may simply produce a video signal with an opposite sign from that due to tunneling. This masking effect becomes more important near visible frequencies because the absorptivity of the metals becomes greater. The measurements here again suggest that the optimum S/N ratios in the beats between visible lasers with large frequency differences will be obtained with the use of operational resistances of about 300  $\Omega$ . This is larger than those used in previous experiments.<sup>1,7</sup>

## CONCLUSIONS

The experimental results reported in the present paper open new possibilities for practical applications of the point contact MIM diodes. In fact, because of the increased radii of the tip, the diodes are dramatically more stable and can be adjusted with more precision without appreciable loss of response times when used in harmonic generation and mixing experiments. The conical configuration is simpler and the focusing geometry, by means of a parabolic mirror, is practical and broadband. The combination of speed, broadband response, and high detectivity of this nonlinear detector is unique. For instance, in the far infrared the sensitivity is comparable to that of a Golay cell, but the speed of response is twelve orders of magnitude faster!

## ACKNOWLEDGMENTS

One of us (M. I.) wishes to thank the Fulbright Program for providing financial support and has greatly appreciated the very warm hospitality of all the members of the Laser Metrology Group at NBS. The authors would like to acknowledge the contributions of F. R. Petersen who passed away December 7, 1983 before the completion of this final version.

- <sup>1</sup>K. M. Evenson, D. A. Jennings, and F. R. Petersen, *J. Phys. (Paris)* **42**, 473 (1981).
- <sup>2</sup>T. E. Sullivan, P. H. Cutler, and A. A. Lucas, *Surf. Sci.* **54**, 561 (1976). T. E. Sullivan, A. A. Lucas, and P. H. Cutler, *Appl. Phys.* **14**, 284 (1977).
- <sup>3</sup>N. M. Miskovsky, P. H. Cutler, T. E. Feuchtwang, and A. A. Lucas, *Int. J. Infrared Millimeter Waves* **2**, 739 (1981).
- <sup>4</sup>G. M. Elchinger, A. Sanchez, C. F. Davis, Jr., and A. Javan, *J. Appl. Phys.* **47**, 591 (1976).
- <sup>5</sup>A. Sanchez, C. F. Davis, D. C. Liu, and A. Javan, *J. Appl. Phys.* **49**, 5270 (1978).
- <sup>6</sup>S. M. Faris, T. K. Gustafson, and J. C. Wiesner, *IEEE J. Quantum Electron.* **QE-9**, 737 (1973).
- <sup>7</sup>H. U. Daniel, M. Steiner, and H. Walther, *Appl. Phys.* **25**, 7 (1981).
- <sup>8</sup>L. M. Matarrese and K. M. Evenson, *Appl. Phys. Lett.* **17**, 8 (1970).
- <sup>9</sup>K. M. Evenson, J. S. Wells, F. R. Petersen, B. L. Danielson, and G. W. Day, *Appl. Phys. Lett.* **22**, 192 (1973).
- <sup>10</sup>J. Ch. Bolomey, J. Cashman, S. El Habiby, and D. Lesselier, *Int. J. Infrared Millimeter Waves* **2**, 859 (1981).
- <sup>11</sup>The mixing order is determined from the expression  $\nu_B = \Sigma m_i \nu_i$ , where  $m_i$  is the harmonic of the  $i$ th oscillator,  $\nu_i$  is the frequency of the  $i$ th oscillator,  $\nu_B$  is the rf beat frequency and  $\Sigma m_i$  is the mixing order.
- <sup>12</sup>M. Inguscio, F. Strumia, K. M. Evenson, and F. R. Petersen, *Seventh International Conference on Infrared and Millimeter Waves*, 14–18 February, Marseille, France (1983).